Application of Box–Behnken design for modeling of lead adsorption onto unmodified and NaCl-modified zeolite NaA obtained from biosilica

Pinar Terzioğlu, Sevil Yücel and Mehmet Öztürk

ABSTRACT

The main objective of the present study was to optimize lead adsorption onto zeolite NaA. For this purpose, to synthesize zeolite NaA under hydrothermal conditions, local wheat husk was precleaned with chemical treatment using hydrochloric acid solution. The unmodified (ZU) and NaCl-modified (ZN) zeolites were characterized by Brunauer–Emmett–Teller, scanning electron microscopy coupled with energy dispersive spectroscopy and X-ray diffraction. The optimization of adsorption process was examined using Box–Behnken Experimental Design in response surface methodology by Design Expert Version 7.0.0 (Stat-Ease, USA). The effects of initial lead (II) concentration, temperature, and time were selected as independent variables. Lack of fit test indicates that the quadratic regression model was significant with the high coefficients of determination values for both adsorbents. Optimum process conditions for lead (II) adsorption onto ZU and ZN were found to be 64.40 °C and 64.80 °C, respectively, and 90.80 min, and 350 mg L^{-1} initial lead(II) concentration for both adsorbents. Under these conditions, maximum adsorption capacities of ZU and ZN for lead (II) were 293.38 mg g^{-1} and 321.85 mg g^{-1}, respectively.

Key words | adsorption, lead, response surface methodology, wheat husk ash, Zeolite A

Pinar Terzioğlu (corresponding author)
Mehmet Öztürk
Department of Chemistry, Faculty of Science,
Muğla Sıtkı Koçman University,
Kötekli 48000,
Turkey
E-mail: *pinarterzioglu86@gmail.com*

Sevil Yücel
Department of Bioengineering, Faculty of Chemistry and Metallurgy,
Yildiz Technical University,
Esenler,
Istanbul 34210,
Turkey

INTRODUCTION

Zeolites hydrated crystalline aluminum silicate solids have attracted more attention due to having wide industrial applications, especially in chemical separation processes as sorbents and catalysts (Azizi *et al.* 2013). Usually, zeolites are categorized into natural and synthetic groups. To date, approximately 213 types of synthetic zeolite were defined by the International Zeolite Association. Synthetic zeolites are preferred because of having controllable properties such as surface area, pore size, and porosity. Among the synthetic zeolites, zeolite NaA offers the greatest potential for separation processes, and shape-selective catalysis makes it commercially significant (Loiola *et al.* 2012). Moreover, zeolite NaA is a low silicon to aluminum ratio zeolite that has high cation exchange capacity.

Wheat husk ash, the byproduct of agricultural based industry, is primarily composed of amorphous silica and other minerals such as calcium, iron, potassium, magnesium and sodium (Terzioğlu *et al.* 2013). Wheat husk ash engenders a disposal problem on account of having no convenient treatment methodology. Currently, Terzioglu *et al.* evaluated the wheat husk ash as a low-cost silica source for the synthesis of barium, calcium and magnesium silicate (Terzioğlu & Yucel 2012; Terzioğlu *et al.* 2013). The previous studies have shown that it is possible to use wheat husk as a practical silica source. Therefore, wheat husk ash rich in amorphous silica is suitable for recycling to synthesize porous materials such as zeolites.

Lead is one of the highly toxic heavy metals brought into aquatic ecosystems by various industrial streams, such as lead-acid battery manufacturing, construction, electronic, fossil fuel, paint, metal phosphate fertilizer, and metal plating. Lead causes several health problems including anemia, chills, diarrhea, headache, and also damaging of the central nervous and reproductive systems (Singh *et al.* 2008). The removal of lead from wastewater streams has significance for the protection of public health (Azizi *et al.* 2013). To eliminate adverse effects of lead, various removal techniques have been investigated. Among them, adsorption

doi: 10.2166/wst.2016.526

has been proposed as an alternative treatment due to its better performance, the presence of several adsorbents with low cost, simple handling and short operation time (Ramakul *et al.* 2012). Zeolites are widely used as adsorbents to remove heavy metals from wastewaters (Kaya & Oren 2006; Nibou *et al.* 2010; Ali *et al.* 2011; Azizi *et al.* 2013).

Experimental design is very helpful to understand better and improve process efficiency that gives information about the interactive effects of the several factors affecting the response (Madala *et al.* 2015). Nowadays, the Box–Behnken design is being adopted to optimize the adsorption processes which is the most frequently used combination design of the response surface methodology (RSM) model (Murugesan *et al.* 2014). The requirement of fewer experiments against other RSM designs is the primary advantage of the Box–Behnken design.

In this study, zeolite NaA was prepared from wheat husk silica and modified with sodium chloride. The adsorbents were characterized via different techniques such as Brunauer–Emmett–Teller (BET), scanning electron microscopy-energy dispersive spectroscopy (SEM-EDS), and X-ray diffraction (XRD). The main goal of the study was to investigate the application of Box–Behnken design to predict adsorption capacity of zeolite NaA samples for the removal of lead (Pb(II)) ions from aqueous solution. The operating conditions were optimized as a function of the initial Pb(II) ions concentration, temperature, and time.

EXPERIMENTAL

Materials

The sodium hydroxide (NaOH), hydrochloric acid (HCl), lead (II) nitrate ($Pb(NO_3)_2$) and sodium aluminate ($NaAlO_2$) were purchased from Sigma-Aldrich (Steinheim, Germany). The wheat husk samples as a precursor of bio-silica were provided from Doruk Marmara Flour Factory, Tekirdağ, Turkey. Deionized water was used to prepare all the solutions.

Synthesis of adsorbents

Synthesis of zeolite NaA (ZU) was carried out according to the procedure that was mentioned in our previous study with the modification of crystallization time as four days (Terzioğlu *et al.* 2016). To prepare NaCl modified sample (ZN), 10 g of ZU was added to 100 mL of NaCl solution (1 mol L^{-1}) and stirred for 24 h. The zeolite was washed with deionized water and dried overnight at 105 °C.

Characterization of adsorbents

BET analysis (NOVA 2200e Quantachrome) was carried out to determine average pore diameter, specific and micro pore surface area, total and micro pore volume of zeolites after degassing at 120 °C for 4 h. SEM images of both zeolite samples were taken, using JEOL JSM-7600 F. XRD analysis was performed to investigate the chemical composition and crystal structure of zeolites on a Philips Panalytical X'Pert Pro, The Netherlands, with CuKα using an acceleration voltage of 45 kV and a current of 40 mA over a range $5^\circ < 2\theta < 90^\circ$ with step size 0.03.

Adsorption studies

The adsorption experiments were performed by using batch equilibration methods. In typical adsorption experiments, 100 mg of zeolite was added to 100 mL of a Pb(II) nitrate aqueous solution in 250 mL conical flasks. Adsorption experiments were investigated at three different temperatures (25, 45 and 65 °C), times (40, 80 and 120 min) and initial Pb(II) concentration (150, 250 and 350 mg L^{-1}) at pH 5.5. During the adsorption, the pH of the suspension was fixed at pH 5.5 by adding NaOH (0.1 N) or HCl (0.1 N) solution. The suspensions were shaken at 160 rpm using a water bath (Memmert WBN 7–45). A stock solution (1,000 mg L^{-1}) was prepared by dissolving analytical reagent grade $Pb(NO_3)_2$ (Sigma-Aldrich) in distilled water. The desired concentration of Pb(II) was prepared by diluting the stock solution (1,000 mg L^{-1}). After each adsorption experiment, the zeolite was separated from aqueous solution by a polytetrafluoroethylene (PTFE) syringe filters (0.45 μm). The residual lead concentration was determined by atomic absorption spectrometry (AAS) using an Agilent 240FS AA Fast Sequential Atomic Absorption Spectrometer with an air-acetylene flame (2.00/13.50 L min^{-1}) and a hollow cathode lamp at 217 nm. The adsorption capacities of the zeolites were calculated according to the following equation:

$$q = \frac{(C_o - C_e) \times V}{m}$$

where q is the adsorption capacity at equilibrium (mg g^{-1}), V is the volume of the solution (L), m is the weight of adsorbent (g), C_o and C_e are the initial and final concentration

of Pb(II) (mg L^{-1}), respectively. All experiments were conducted three times, and arithmetic averaged results were presented.

Box–Behnken experimental design

The three level, three factorial Box–Behnken experimental design containing five replicates at the center point was used to unearth the optimum conditions for maximum Pb(II) adsorption by zeolite NaA. For statistical calculations, the three independent variables were designed as temperature (x_1), time (x_2) and initial Pb(II) concentration (x_3) with the coded values at three levels as −1 (low), 0 (central point), and +1 (high). Analysis of variance (ANOVA) with the help of Design Expert software was used to determine the interaction between design variables and the response. Model terms were chosen when *p*-value (probability) was with a 95% confidence limit.

RESULTS AND DISCUSSION

Characterization of adsorbents

SEM micrographs of zeolite NaA samples are given in Figure 1. The ZU and ZN crystals were round-like with a particle size of 2.28–2.93 μm and 1.0–1.89 μm, respectively. The particle size of ZU was decreased after NaCl modification process.

Table 1 shows the elemental compositions of ZU and ZN samples. The SEM-EDS results showed that silicon to aluminium ratio of zeolites was 1:1.06 confirming the production of zeolite NaA. The Na content of ZN was 116.35% more than ZU.

The surface area of ZN sample (5.87 $m^2 g^{-1}$) was found to be higher than ZU sample (2.75 $m^2 g^{-1}$). In accordance with the previous publication (Lin *et al.* 2013), a significant increment in the average pore diameter, surface area and total pore volume of zeolite was observed after the sodium treatment (Table 2).

The XRD patterns of zeolite NaA and the NaCl-modified zeolite NaA are presented in Figure 2. The XRD patterns revealed that the major phase in the zeolites was zeolite A ($Na_{92.71}(Si_{96.96}\ Al_{95.04}\ O_{384})(H_2O)_{254.64}$) and the minor phase sodium aluminum silicate hydrate ($Na_8Si_6Al_6O_{24}(OH)_2(H_2O)_2$). From the XRD patterns, no significant changes in the positions were determined, but the intensity of diffraction peaks showed differences. The present findings show that the crystal structure of ZU was not distorted after NaCl modification process. Similar results were found by Baskan & Pala (2011).

Specification of the regression model and statistical analysis

A well-fitted regression model of adsorption process was determined by statistical analysis. The Box–Behnken design matrix together with observed and predicted experimental response values are summarized in Table 3. The following second-order polynomial equation were performed to find out the Pb(II) sorption capacity of ZU and ZN, respectively:

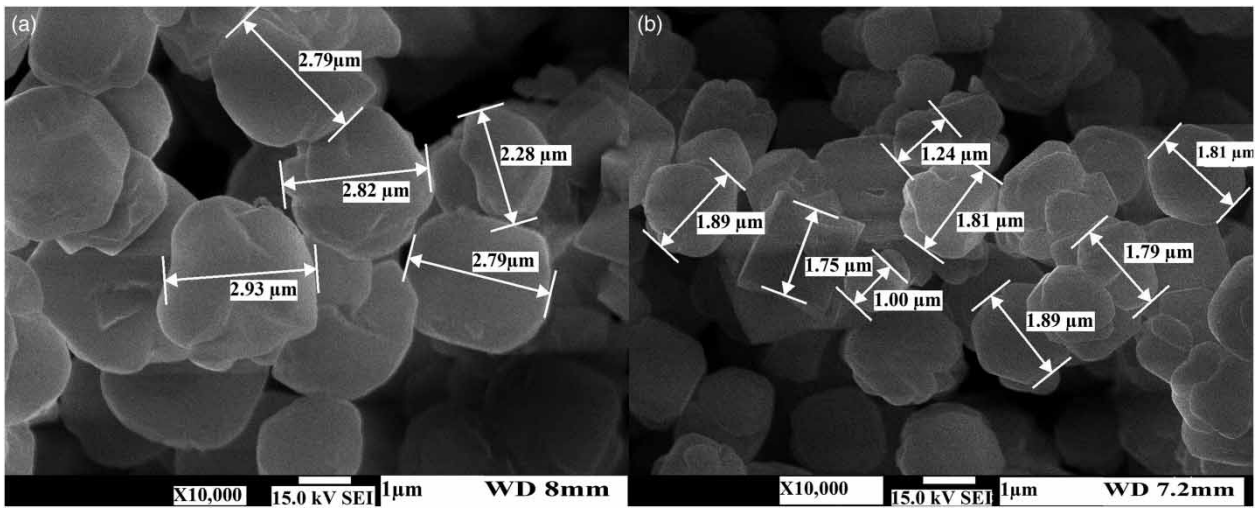

Figure 1 | SEM micrographs of (a) ZU and (b) ZN (×10,000).

Table 1 | The average elemental composition of ZU and ZN samples

Element (%,atomic)	ZU	ZN	Zeolite NaA[a]
Si	11.91	11.50	10.80
Al	11.16	10.84	10.80
Na	12.11	14.09	10.80
O	64.49	63.22	67.60
Au	0.33	0.35	–
Si/Al	1.06	1.06	1.00

[a]Calculated from the chemical formula of zeolite NaA.

Table 2 | The surface area, average pore diameter and total pore volume of ZU and ZN samples

	ZU	ZN
BET surface area ($m^2\ g^{-1}$)	2.75	5.87
Total pore volume ($cm^3\ g^{-1}$)	0.002	0.018
Average pore diameter (nm)	17.66	45.75

$$q_{ZU} = 218.37800 + 10.66875\ \ x_1 + 3.28125\ \ x_2 + 77.16250\ \ x_3 - 0.91750\ \ x_1x_2 + 4.11500\ \ x_1x_3 - 0.39500\ \ x_2x_3 - 6.67275\ \ x_1^2 - 4.17275\ \ x_2^2 - 10.33025\ \ x_3^2 \quad (1)$$

$$q_{ZN} = 238.51800 + 11.48125\ \ x_1 + 4.41625\ \ x_2 + 77.55500\ \ x_3 + 1.70750\ \ x_1x_2 + 8.27000\ \ x_1x_3 - 1.79500\ \ x_2x_3 + 1.53725\ \ x_1^2 - 9.61775\ \ x_2^2 - 15.71525\ \ x_3^2 \quad (2)$$

where q_{ZU} and q_{ZN} are the predicted responses for the Pb(II) removal capacity of adsorbate, and x_1, x_2 and x_3 are the coded values of independent variables, temperature, time and initial Pb(II) concentration, respectively. As can be seen from Table 3, Pb(II) uptake capacities were in the range of 140.76–321.33 mg g^{-1} for ZN and 118.13–292.85 mg g^{-1} for ZU. It can be pointed out that ZN has greater Pb(II) adsorption capacity than ZU.

The ANOVA is necessary to examine the significance and the fit of the second-order polynomial equation (Yetilmezsoy *et al.* 2009). Results of ANOVA for the model used to predict Pb(II) uptake on each adsorbate were given in Table 4. The regression models indicated that the quadratic model was highly significant, as was evident from the high value of Fisher variation ratio ($F_{model\ ZU} = 5333.27$, $F_{model\ ZN} = 5257.66$) with a very low probability value ($p < 0.0001$). The

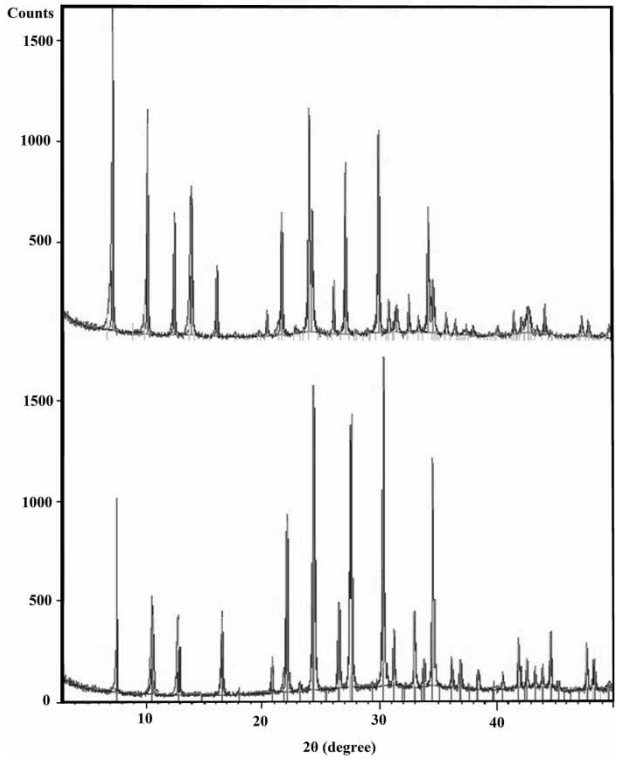

Figure 2 | XRD patterns of (a) ZU and (b) ZN.

tabulated F-value for ZU and ZN were found to be 47.74 and 32.32, respectively. It can be concluded that the treatment combinations had statistical significance since the tabulated F-values were smaller than the calculated F-values. Adequate precision ratios were 225.581 and 241.118 for Pb(II) adsorption models with ZU and ZN, respectively, showed the presence of the adequate signal to noise due to being much greater than the least desirable amount of 4.0 (Ahmadi *et al.* 2014).

Smaller *p*-values ($p < 0.05$) imply the significance of each coefficient (Table 4). It was determined that the first-order main effects of all three variables, temperature (x_1), time (x_2), and concentration (x_3) were highly significant ($p < 0.0001$). Furthermore, very small respective *p*-values of the second-order main effects of all three variables (x_1^2, x_2^2, x_3^2) indicated that they were also significant. The interactive effects of temperature and time, temperature and concentration, concentration and time were also significant for adsorption onto ZN. However, the interactive effects of temperature and time, concentration and time for adsorption onto ZU were insignificant since the *p*-value were higher than 0.05.

The goodness of fit of the models was stated by the value of determination coefficient (R^2). The R^2_{adj} and R^2 were closed to each other represented that there are not any excessive

Table 3 | The Box–Behnken design matrix and the comparison of observed and predicted results for the adsorption of Pb(II) ion onto ZU and ZN

				Sorption capacity (q, mg g^{-1})			
	Independent variables			ZN		ZU	
Run	Temperature (x_1, °C)	Time (x_2,minute)	Concentration (x_3, mg L^{-1})	Observed	Predicted	Observed	Predicted
1	25	40	250	215.16	216.25	192.25	192.67
2	65	40	250	235.03	235.80	217.01	215.84
3	25	120	250	222.43	221.67	199.89	201.06
4	65	120	250	249.13	248.04	220.98	220.57
5	25	80	150	143.89	143.57	118.13	117.66
6	65	80	150	149.99	150.00	129.65	130.77
7	25	80	350	282.15	282.14	264.87	263.75
8	65	80	350	321.33	321.65	292.85	293.32
9	45	40	150	130.19	129.42	122.98	123.04
10	45	120	150	140.76	141.84	131.09	130.39
11	45	40	350	289.20	288.12	277.45	278.15
12	45	120	350	292.59	293.36	283.98	283.92
13	45	80	250	238.31	238.52	218.24	218.38
14	45	80	250	238.45	238.52	218.65	218.38
15	45	80	250	238.99	238.52	218.32	218.38
16	45	80	250	238.35	238.52	218.12	218.38
17	45	80	250	238.45	238.52	218.65	218.38

Table 4 | ANOVA results of the regression model for optimization of Pb(II) adsorption

	Sum of squares			Mean square		F value		*p*-value	
Factors	ZU	ZN	d_f	ZU	ZN	ZU	ZN	ZU	ZN
Model	49480.96	51127.49	9	5497.88	5680.83	5333.27	5257.66	<0.0001	<0.0001
x_1	910.58	1054.55	1	910.58	1054.55	883.31	976.00	<0.0001	<0.0001
x_2	86.13	156.03	1	86.13	156.03	83.55	144.40	<0.0001	<0.0001
x_3	47632.41	48118.22	1	47632.41	48118.22	46206.26	44533.85	<0.0001	<0.0001
x_1 x_2	3.37	11.66	1	3.37	11.66	3.27	10.79	0.1137	0.0134
x_1x_3	67.73	273.57	1	67.73	273.57	65.70	253.19	<0.0001	<0.0001
x_2x_3	0.62	12.89	1	0.62	12.89	0.61	11.93	0.4620	0.0106
x_1^2	187.48	9.95	1	187.48	9.95	181.86	9.21	<0.0001	0.0190
x_2^2	73.31	389.48	1	73.31	389.48	71.12	360.47	<0.0001	<0.0001
x_3^2	449.32	1039.87	1	449.32	1039.87	435.87	962.41	<0.0001	<0.0001
Residual	7.22	7.56	7	1.03	1.08				
Lack of fit	7.02	7.26	3	2.34	2.42	47.74	32.32	0.0014	0.0029
Pure error	0.20	0.30	4	0.049	0.075				
Cor total	49488.18	51135.05	16						

ZU, ZN: $R^2 = 0.9999$ and $R^2_{Adj} = 0.9997$.

variables. The determination coefficient values of 0.9999 for both adsorbents signified the good fitness of regression models for predicting the Pb(II) sorption capacity results. The high value of R^2_{adj} (0.9997) indicated a high significance of the model (Can *et al.* 2006). Additionally, the coefficient of variation ($CV_{ZU} = 0.49\%$, $CV_{ZN} = 0.46\%$) values were low due to a good deal of the credibility of the performed experiments and the extremely high degree of precision (Yetilmezsoy *et al.* 2009).

The numerical analysis of the response surface was applied to evaluate the optimum process conditions. The optimum level of variables for Pb(II) adsorption were found to be 64.40 °C, 90.80 min and 350 mg L^{-1} initial concentration with 293.38 mg g^{-1} sorption capacity by ZU, while optimum conditions for ZN with 321.85 mg g^{-1} sorption capacity were 64.80 °C, 90.80 min and 350 mg L^{-1} initial Pb(II) concentration.

Effect of process variables on Pb(II) adsorption

The three-dimensional (3D) response surface plots are very useful in order to analyze the relationship between the three important variables and response (Yetilmezsoy *et al.* 2009; Simsek *et al.* 2013). Hence, the response surface plots were given in Figures 3 and 4 to gain a better understanding.

Effect of temperature

The effect of temperature on Pb(II) adsorption capacities of samples can be deduced from Figures 3(a), 3(b) and 4(a), 4(b). In the present study, the adsorption experiments were carried out at different temperatures ranging from 25 to 65 °C. It was determined that increasing the temperature increases the adsorption capacities of both samples. The equilibrium Pb(II) adsorption capacity of ZU rise from 192.25 mg g^{-1} at 25 °C (run number 1) to 217.01 mg g^{-1} at 65 °C (run number 2). The increment of Pb(II) adsorption capacity of ZN with the increase of temperature was clearly in agreement with that of ZU. Similarly, Buasri *et al.* (2008) reported that Pb(II) adsorption capacity of natural clinoptilolite was increased from 50 mg g^{-1} at 30 °C to 58.75 mg g^{-1} at 75 °C. These observations demonstrated that the adsorption process had an endothermic behavior for both samples. The provided results of this study agree with the results previously found for the uptake of Pb(II)

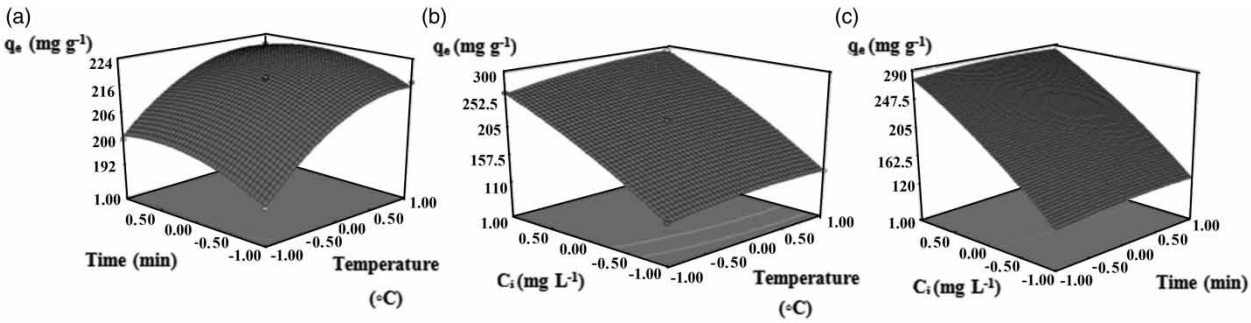

Figure 3 | 3D response surface plots exhibiting the interactive effects of (a) temperature (x_1) and time (x_2), (b) temperature (x_1) and initial concentration of Pb(II) ions (C_i, x_3), (c) initial concentration of Pb(II) ions (C_i, x_3) and time (x_2), on adsorption capacity of ZU.

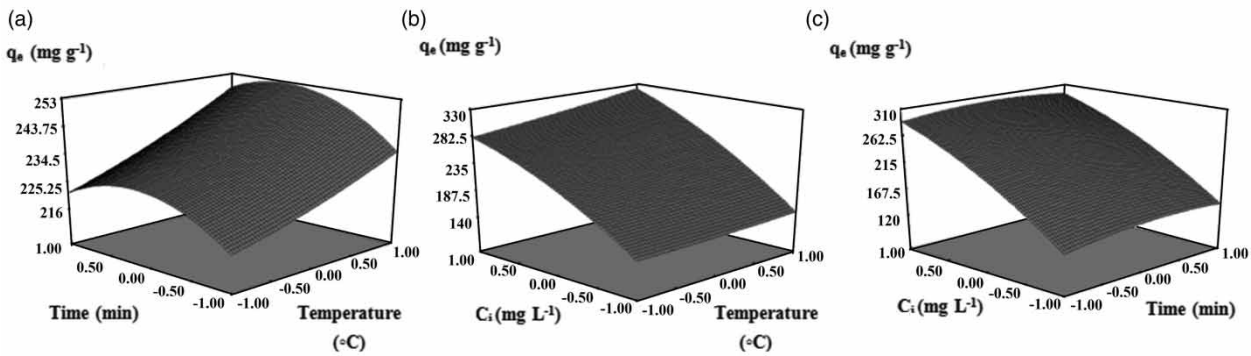

Figure 4 | 3D response surface plots exhibiting the interactive effects of (a) temperature (x_1) and time (x_2), (b) temperature (x_1) and initial concentration of Pb(II) ions (C_i, x_3), (c) initial concentration of Pb(II) ions (C_i, x_3) and time (x_2), on adsorption capacity of ZN.

ions by various adsorbents as active carbon (Mengistie *et al.* 2008), carbon aerogel (Goel *et al.* 2005) and clinoptilolite (Buasri *et al.* 2008).

Effect of contact time

The uptake of Pb(II) by zeolites was examined at different time intervals ranging from 40 to 120 min. Variations of Pb(II) adsorption capacities of samples with time can be inferred from Figures 3(a), 3(c) and 4(a), 4(c). Increasing the contact time from 40 to 120 min increased the percentage removal of Pb(II) ions by zeolites. During the first 40 min, rapid uptake of Pb(II) was noticed. From 40 to 120 min, the Pb(II) uptake increased and reached equilibrium at around 120 min (Table 3). This view is supported by the findings of Huang *et al.* (2015).

Effect of initial Pb(II) concentration

Lead(II) adsorption onto zeolites was carried out at three levels of initial Pb(II) concentrations, ranging from 150 to 350 mg L^{-1}. Figures 3(b), 3(c) and 4(b), 4(c) show the effect of the initial Pb(II) concentration on the uptake capacity of ZU and ZN. In this case, initial Pb(II) concentration had a prominent favorable influence on the quantity of Pb(II) adsorbed onto both samples. In the performed initial Pb(II) concentration range, the maximum Pb(II) uptake capacity was achieved at the maximum Pb(II) concentration of 350 mg L^{-1}. This can be explained by the fact that at higher concentrations there is a higher probability of collision between active sides of adsorbents and heavy metal ions base on the higher mobility of ions and fast diffusion (Avcı Tuna *et al.* 2013). The adsorption capacities of ZU were 118.13, 192.25 and 264.87 mg g^{-1} for initial Pb(II) concentration of 150, 250 and 350 mg L^{-1}, respectively. Adsorption capacities of ZN were obtained as 143.89, 215.16 and 282.15 mg g^{-1} for initial Pb(II) concentration of 150, 250 and 350 mg L^{-1}, respectively.

CONCLUSIONS

In this study, application of biosilica based zeolites for adsorption of lead ions was investigated by an RSM with the Box–Behnken design. Temperature (25–65 °C), contact time (40–120 min) and initial Pb(II) concentration (150–350 mg L^{-1}) were chosen as the independent variables. The amount of Pb(II) ions adsorbed onto zeolites increased with the increasing initial concentration, temperature and prolonged contact time. The ANOVA results clearly suggests that the adsorption of Pb(II) ion onto zeolite samples was highly significant based on very low *p*-values. ZN is a more efficient adsorbent for the adsorption of Pb(II) from aqueous solution when compared with ZU. Summarizing, the reduction of cost by utilizing waste materials and comparatively simple evaluation of the influence of process parameters makes adsorption of Pb(II) ion from aqueous solutions economically feasible.

ACKNOWLEDGEMENTS

This study was supported by the Scientific Research Projects of the Yıldız Technical University, Istanbul, Turkey under project number 2014-07-04-DOP02. Mugla Sitki Kocman University Scientific Research Fund with the project number 12/135 is also acknowledged.

REFERENCES

Ahmadi, A., Heidarzadeh, S., Mokhtari, A. R., Darezereshki, E. & Harouni, H. A. 2014 Optimization of heavy metal removal from aqueous solutions by maghemite (γ-Fe_2O_3) nanoparticles using response surface methodology. *Journal of Geochemical Exploration* **147**, 151–158.

Ali, I. O., Hassan, A. M., Shaaban, S. M. & ve Soliman, K. S. 2011 Synthesis and characterization of ZSM-5 zeolite from rice husk ash and their adsorption of Pb^{2+} onto unmodified and surfactant-modified zeolite. *Separation and Purification Technology* **83**, 38–44.

Avcı Tuna, A. Ö., Özdemir, E., Simsek, E. B. & Beker, U. 2013 Optimization of process parameters for removal of arsenic using activated carbon-based iron-containing adsorbents by response surface methodology. *Water, Air, and Soil Pollution* **224**, 1685.

Azizi, S. N., Dehnavi, A. R. & Joorabdoozha, A. 2013 Synthesis and characterization of LTA nano zeolite using barley husk silica: mercury removal from standard and real solutions. *Materials Research Bulletin* **48**, 1753–1759.

Baskan, M. B. & Pala, A. 2011 Removal of arsenic from drinking water using modified natural zeolite. *Desalination* **281**, 396–403.

Buasri, A., Chaiyut, N., Phattarasirichot, K., Yongbut, P. & Nammueng, L. 2008 Use of natural clinoptilolite for the removal of lead (II) from wastewater in batch experiment. *Chiang Mai Journal of Science* **35** (3), 447–456.

Can, M. Y., Kaya, Y. & Algur, O. F. 2006 Response surface optimization of the removal of nickel from aqueous solution by cone biomass of *Pinus sylvestris*. *Bioresource Technology* **97**, 1761–1765.

Goel, J., Kadirvelu, K., Rajagopal, C. & Garg, V. K. 2005 Removal of lead(II) from aqueous solution by adsorption on carbon

aerogel using a response surface methodological approach. *Industrial and Engineering Chemical Research* **44**, 1987–1994.

Huang, G., Wang, D., Ma, S., Chen, J., Jiang, L. & Wang, P. 2015 A new, low-cost adsorbent: preparation, characterization, and adsorption behavior of Pb(II) and Cu(II). *Journal of Colloid and Interface Science* **445**, 294–302.

Kaya, A. & Oren, A. H. 2006 Factors affecting adsorption characteristics of Zn^{2+} on two natural zeolites. *Journal of Hazardous Materials* **B131**, 59–65.

Lin, L., Lei, Z., Wang, L., Liu, X., Zhang, Y., Wan, C., Lee, D. J. & Tay, J. H. 2013 Adsorption mechanisms of high-levels of ammonium onto natural and NaCl-modified zeolites. *Separation and Purification Technology* **103**, 15–20.

Loiola, A. R., Andrade, J. C. R. A., Sasaki, J. M. & da Silva, L. R. D. 2012 Structural analysis of zeolite NaA synthesized by a cost-effective hydrothermal method using kaolin and its use as water softener. *Journal of Colloid and Interface Science* **367** (1), 34–39.

Madala, S., Reddy, M. V. N., Vudagandla, S. & Abburi, K. 2015 Modified leaf biomass for Pb(II) removal from aqueous solution: application of response surface methodology. *Ecological Engineering* **83**, 218–226.

Mengistie, A. A., Rao, T. S., Rao, A. V. P. & Singanan, M. 2008 Removal of lead(II) ions from aqueous solutions using activated carbon from militia ferruginea plant leaves. *Bulletin of the Chemical Society of Ethiopia* **22** (3), 349–360.

Murugesan, A., Vidhyadevi, T., Kalaivani, S. S., Thiruvengadaravi, K. V., Ravikumar, L., Anuradha, C. D. & Sivanesan, S. 2014 Modelling of lead(II) ion adsorption onto poly(thiourea imine) functionalized chelating resin using response surface methodology (RSM). *Journal of Water Process Engineering* **3**, 132–143.

Nibou, D., Mekatel, H., Amokrane, S., Barkat, M. & Trari, M. 2010 Adsorption of Zn^{2+} ions onto NaA and NaX zeolites: kinetic, equilibrium and thermodynamic studies. *Journal of Hazardous Materials* **173**, 637–646.

Ramakul, P., Yanachawakul, Y., Leepipatpiboon, N. & Sunsandee, N. 2012 Biosorption of palladium (II) and platinum(IV) from aqueous solution using tannin from Indian almond (*Terminalia catappa* L.) leaf biomass: kinetic and equilibrium studies. *Chemical Engineering Journal* **193–194**, 102–111.

Simsek, E. B., Özdemir, E. & Beker, U. 2013 Process optimization for arsenic adsorption onto natural zeolite incorporating metal oxides by response surface methodology. *Water, Air, and Soil Pollution* **224**, 1614.

Singh, C. K., Sahu, J. N., Mahalik, K. K., Mohanty, C. R., Mohan, B. R. & Meikap, B. C. 2008 Studies on the removal of Pb(II) from wastewater by activated carbon developed from Tamarind wood activated with sulphuric acid. *Journal of Hazardous Materials* **153** (1–2), 221–228.

Terzioglu, P. & Yucel, S. 2012 Synthesis of magnesium silicate from wheat husk ash: effects of parameters on structural and surface properties. *BioResources* **7** (4), 5435–5447.

Terzioğlu, P., Yucel, S. & Özçimen, D. 2013 The utilization of wheat hull ash for the production of barium and calcium silicates. *Latin American Applied Research* **43** (4), 319–324.

Terzioğlu, P., Yucel, S. & Öztürk, M. 2016 Synthesis of zeolite NaA from a new biosilica source. *Waste and Biomass Valorization* **7** (5), 1271–1277.

Yetilmezsoy, K., Demirel, S. & Vanderbei, R. J. 2009 Response surface modeling of Pb(II) removal from aqueous solution by *Pistacia vera* L.: Box-Behnken experimental design. *Journal of Hazardous Materials* **171**, 551–562.

First received 20 June 2016; accepted in revised form 31 October 2016. Available online 15 November 2016